A Study of Seismic Behavior of Transmission Tower Foundations During the 2011 Tohoku Earthquake

Y. Tamari Y. Nakagama, M. Kikuchi, M. Morohashi, T. Kurita, Y. Shingaki,
Y. Hirata, R. Ohnogi, H. Nakamura
Tokyo Electric Power Services Co., Ltd. Tokyo, Japan

ABSTRACT
The massive 11 March 2011 earthquake that occurred off the coast of Tohoku, Japan had a magnitude of 9.0 with long duration. This caused widespread accidents to occur in the electric power infrastructure of the Kanto region, which encompasses Tokyo. The cause of the damage was not easily understood, especially concerning the short-circuit accident, which is due to contact of electric wires during the earthquake. To clarify the cause of event, Ohta et al. (2014) conducted numerical analysis using a model of transmission towers with electric wires. They suggested that the contact of electric wires could occur when difference of earthquake response between two foundations are significant. To examine the seismic behavior of foundations, we took the ground and foundation conditions into account and conducted soil foundation coupled analysis by the effective stress analysis. It was found that different earthquake response between foundations in terms of horizontal displacement and rotation of foundation could occur during the main shock of the earthquake.

1 INTRODUCTION

The massive 11 March 2011 Tohoku earthquake that occurred off the coast of Tohoku (northeast), Japan (hereafter, Earthquake 3.11) had a magnitude of 9.0 with a long duration of more than 300 seconds. This caused widespread accidents to occur in the electric power infrastructure of the Kanto region, which encompasses Tokyo. The cause of occurrence of the accidents were not fully understood, especially concerning the short-circuit accidents, which was likely due to the contact of transmission wires by earthquake excitation.

To clarify the cause of the event, Ohta et al. (2014) conducted a structural numerical analysis using a simulation model with transmission towers and electric wires. They found that the contact of wires could occur when phase difference of horizontal displacement between foundations of transmission towers exceeds 0.7 seconds. In addition, they assumed that the event may possibly occur due to a combination of various factors as such the duration of the earthquake, structure of the transmission towers, earthquake waves, topological condition, and soil profile around the transmission towers.

Following their assumptions in this study, in order to try to clarify the phenomenon we focused not only on the structure but also on the surrounding ground and the pile foundations. It is important to consider the effects of i) the foundations and ground conditions at the subsurface, including soil liquefaction, ii) the basin terrain and topological condition at the site, iii) and the difference of velocity structure in the deep parts of ground between the foundations.

For the study the authors began by conducting three dimensional effective stress dynamic analyses considering soil-structure interaction for two transmission tower foundations in order to examine occurrence of phase difference between foundations. Since potential of soil liquefaction was reported around the one side of transmission tower by regional government (Yamanashi Prefecture, 2013), the pore water build-up was considered in sandy soil layer. The model used for soil in this study is an extended strain space multiple mechanism model into three dimensional space (Iai, 1993). It is based on a plane strain mechanism (Iai et al., 1992), which has been commonly used for the performance based design of various structures in Japan.

2 BRIEF REVIEW OF PAST STRUCTURAL ANALYSIS

The transmission towers which Ohta et al.(2014) studied are located in the southern part of Kofu basin, Yamanashi Prefecture, Japan. Location in detail is illustrated in Figure 1.

Ohta et al. (2014) conducted the event reproduction analysis using the model composed of four towers and three spans both ground wire and electric wires as shown in Figure 2. The place where short-circuiting occurred during the Earthquake 3.11 is marked in the figure. The span between tower no.2 and no.3 was 440m, in which natural period of first mode for electric wire at the span was 7.87 seconds. Damping ratio of 0.4% for electric wire was considered in the analysis. Program ADINA ver.8.8 (2011) was used for the analysis by taking the geometrical nonlinearity of electric wires into account.

The observed motion at the recording station “YMN005” (2011/03/11-14:46, 38.103N, 142.860E, M9.0, K-NET: NIED), which was about 7km north of the site, was directly applied to the model. Since it was thought that the phase difference between towers which occurred during the earthquake had several causes, they conducted the analysis by varying the phase difference of input motion between the foundations from 0 seconds to 5 seconds. The results of the analysis were summarized as follows:

(i) The contact of electric wire which might cause a short-circuit was successfully reproduced when the phase differences of 0.7 to 1 second, 3 seconds and 5 seconds were taken into account in the calculation. The contact of electric wires was not simulated with the phase difference of 2 seconds and 4 seconds.

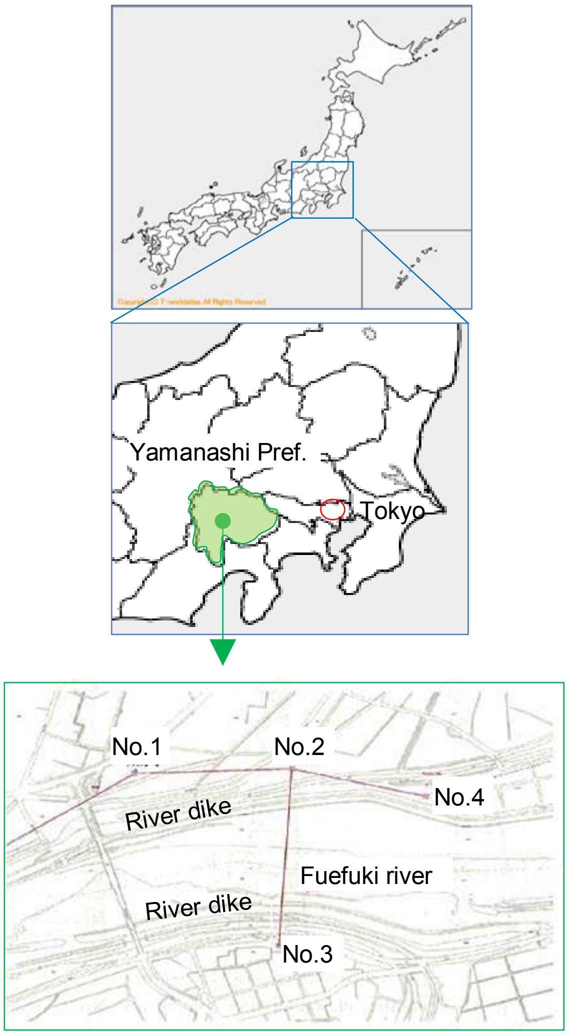

(after Ohta et al. 2014)

Figure 1. Location of Transmission Towers and River area

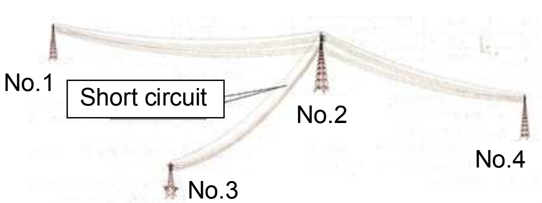

Figure 2. Numerical Analysis Model Composed of 4 towers and 3 span ground and Electric wires (Ohta el al. 2014)

(ii) The calculated location of the contact of electric wires was consistent with the fact evaluation. The motion of electric wires in the vertical direction at that time was in the third or fourth mode rather than the first mode.

(iii) The duration contact of the electric wires was simulated between 140 seconds and 200 seconds, which was roughly in line with the reported result of the event analysis of 120 seconds to 180 seconds.

They concluded that the main cause of the contact was earthquake motion, and indicated the following specific conditions in which the event was likely to occur: i) a long duration of motion, ii) the existence of long period component, and iii) topographic and geotechnical condition which likely produce a phase difference of ground motion.

3 CONSIDERATION ON GROUND CONDITIONS

We examined more details about the conditions of site from a geotechnical point of view referring to various literatures.

3.1 Topography and Deep Ground Velocity Structure

Kofu basin is shown as a reverse triangle in Figure 3 with a length of about 20km in an east-west direction, and 15km in a north-south direction. The basin is regarded as structural basin which is surrounded by mountains in three directions. The elevation of its bottom surface is about 250m to 300m. The site is located at the south tip of lowland of the basin as marked by red circle in the figure. Approximate location of seismic prospecting by Yamanashi regional government (2003) is also depicted in the figure. Figure 4 illustrates geological cross section of Kofu basin along the line of seismic prospecting. The shear wave velocity results, which were evaluated in a past study at each stratum, is written in the legend. Sedimentary stratum and tertiary formation (Vs=1.04km/s) exists underlain by top gravel stratum (Vs=0.42m) with a maximum thickness of about 100m at the surface.

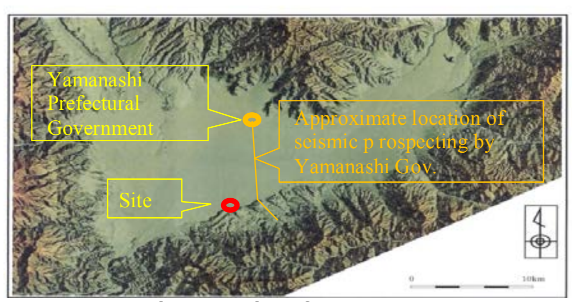

Figure 3. Relief map of Kofu basin (Yamanashi Pref. Japan, 2003)

3.2 Average shear wave velocity (VS30 values)

Figure 5 illustrates VS30 map around the transmission towers (NIED, J-SHIS, 2016).

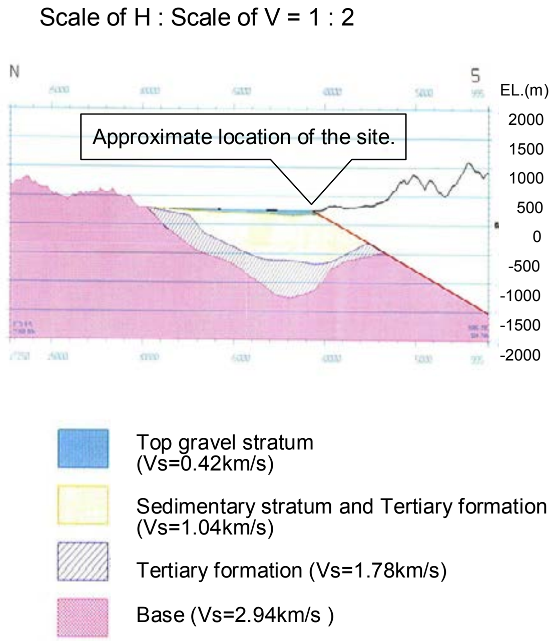

Figure 4. Cross Section of Kofu basin (N-S Direction, Yamanashi Pref. Japan, 2003)

VS30 herein implies average shear wave velocity of surface 30m subsoil. VS30 value around tower no.2 has a range of 160m/s to 200m/s, whereas the value around tower no.3 is about 250m/s to 350m/s. According to the past evaluation of micro topographic classification, this portion of southern side of the river is regarded as alluvial fan (NIED, J-SHIS, 2016).

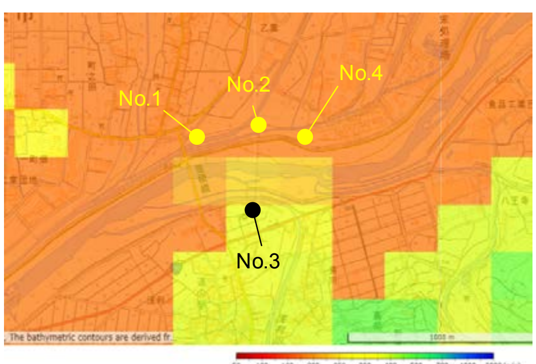

Figure 5. Map of VS30 value (NIED, J-SHIS, 2016)

3.3 Liquefaction Evaluation

Yamanashi Regional Government regularly reports the result of liquefaction evaluations for whole area of Yamanashi prefecture (Yamanashi Prefecture, 2013). Figure 6 shows the distribution of liquefaction potential as PL values (Iwasaki et. al. 1981) around the transmission towers. It is seen that PL value around tower no.2 is more than 15 indicating high possibility of liquefaction occurrence. In contrast with this, the ground surrounding tower no.3 on the south side of the river may not be subject to liquefaction as it has a PL value of 0.

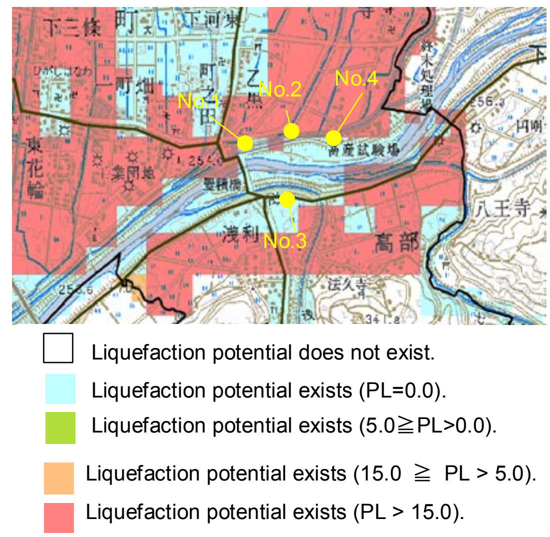

Figure 6. Liquefaction Hazard Map around the site (Yamanashi Pref, 2013)

3.4 Consideration

In light of the above mentioned geotechnical conditions we observe the following points.

(i) As a consequence of the variations in the basin terrain (e.g. the thickness of gravel stratum at the surface of basin (Vs=420m/s) varies between the locations of towers no.2 and no.3, the deep subsurface structure is vary by several hundred meters horizontally. This may cause phase differences in the earthquake response.

(ii) VS30 value is different at surrounding ground between towers no.2 (about 180m/s) and no.3 (about 300m/s). Difference of VS30 value may cause different earthquake responses between foundations such as horizontal motion and rotation of foundation.

(iii) Liquefaction resistance may be lower in subsoil around tower no.2 than around tower no.3. This may cause softening of sandy soil during earthquake with long duration, resulting in long natural period of subsoil around tower no.2.

We consider points of study to clarify the earthquake response between foundations from variety of aspects as:

- the foundation and subsoil system, in consideration of soil liquefaction;
- the difference of VS30 value at each transmission tower; and
- the deep subsoil structure of shear wave velocity and the topography of the basin.

The first point can be considered to conduct soil foundation coupled analysis of transmission tower foundations. The second and third points can be taken into account to conduct numerical analyses of large models, in which both wide areas and deep ground are taken into account.

To start with a series of study, we present in this paper the study by conducting soil foundation coupled with an analysis of liquefaction.

4 SOIL FOUNDATION COUPLED ANALYSIS OF TRANSMISSION TOWERS

4.1 Subsurface Soil Conditions and Model Parameters

Borehole log and N value of standard penetration tests at each tower are shown in Figure 7. The borehole no.2 is located at the foundation of the tower no.2, whereas borehole no.3 is about 150m east from tower no.3, which is opened to the public by Ministry of Land, Infrastructure, Transport and Tourism (MLIT, 2016). Test for particle size distribution were conducted using several number of penetration samples. Fine fraction contents of soils are 7.9% to 37.9% in alluvial sand layer, 47.9% to 80.5% in alluvial clayey layer, 5.4% in alluvial gravel layer. Results of PS logging, cyclic test for dynamic deformation and liquefaction characteristics were not reported.

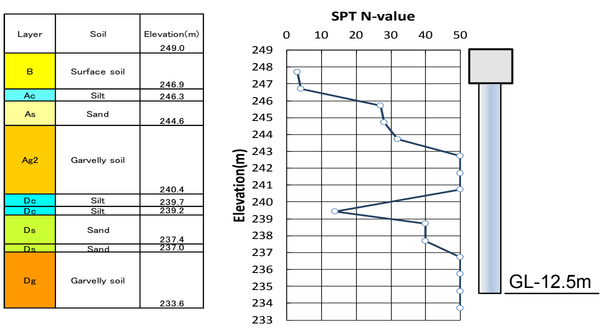

(a) Borehole No.2

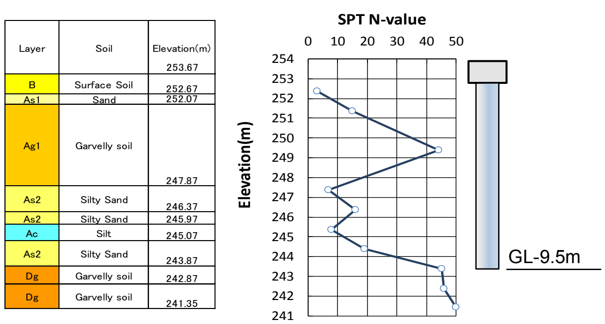

(b) Borehole No.3 (MLIT, KT_2014_02139)

Figure 7. Borehole Log and SPT N-value

The ground models at each tower were developed by referring to boring logs. The layer and thickness is illustrated in Table 1 and Table 2. The model parameters of a strain space multiple shear mechanism for soil (Iai et al., 1992, Iai, 1993) were basically assessed using simplified method (Morita et al., 1997) by referring to SPT N value and fine fraction contents. Shear wave velocity were adjusted considering VS30 values at each foundations. Empirical correlation formula with SPT N value (Cabinet Office, Japan. 2001) was also referred to. Parameters for physical characteristics, dynamic deformation characteristics, liquefaction characteristics are summarized in Table 1 and Table 2. Average shear wave velocity were assumed as 176m/s in no.2 and 285m/s in no.3, being consistent with VS30 values. Dilatancy of soil was taken into account for bank soil material below water table. Parameters for liquefaction were specified as best assessed parameter set by numerical simulation of undrained cyclic shear loading.

Table 1. Ground Model and Parameters for Subsoil (Tower No.2, VS30: about 180m/s)

Layer	H (m)	ρ (t/m^3)	V_s (m/s)	G_{ma} (kPa)	$-\sigma_{ma}'$ (kPa)	φ_f (deg)	h_{max}	φ_p (deg)	Cyc.Str.Ratio DA=5.0%
B	1.4	1.6	132	27950	13.6	39.0	0.24	–	–
B	0.7	1.6	132	27950	13.6	39.0	0.24	28.0	0.188
Ac	0.6	1.5	161	38760	18.0	30.0	0.20	–	–
As	1.7	1.9	180	61560	24.3	43.9	0.24	–	–
Ag2	1.4	2.0	180	64800	35.2	43.9	0.24	–	–
Ag2	2.8	2.1	180	68040	48.5	43.9	0.24	–	–
Dc	1.2	1.8	180	58320	62.3	0.0*1	0.20	–	–
Ds	2.2	1.9	180	61560	71.3	43.8	0.24	–	–
Dg	4.8	2.1	180	68040	95.1	43.9	0.24	–	–

∑H=16.8m $V_{s,ave}$=176m/s *1 Cohesion: 1057 kPa Ground water level: GL-1.4m

Table 2. Ground Model and Parameters for Subsoil (Tower No.3, VS30: about 300m/s)

Layer	H (m)	ρ (t/m^3)	V_s (m/s)	G_{ma} (kPa)	$-\sigma_{ma}'$ (kPa)	φ_f (deg)	h_{max} (deg)	φ_p	Cyc.Str.Ratio DA=5.0%
B	1.0	1.6	132	27950	13.6	39.0	0.24	–	–
As1	0.6	1.6	131	29200	13.8	38.8	0.24	–	–
Ag1	3.0	1.5	241	116450	36.7	43.9	0.24	–	–
Ag1	1.2	1.9	241	116450	36.7	43.9	0.24	–	–
As2	4.0	2.0	190	68920	75.9	40.0	0.24	–	–
Dg	11.7	2.1	354	262480	129.6	43.8	0.24	–	–

∑H=21.5m $V_{s,ave}$=285m/s Ground water level: GL-4.6m

H: layer thickness; *p:* density; V_s :shear wave velocity; G_{ma}: elastic shear modulus at a confining pressure of $(-\sigma_{ma}')$; $-\sigma_{ma}'$: reference confining pressure; φ_f :shear resistance angle; and φ_p :phase transformation angle

4.2 Foundations and Transmission Tower

Each transmission tower has pile foundation with square shaped footing. Approximate depth of footing and pile are illustrated in above mentioned Figure 7. Specification of foundations is summarized in Table 3. The concrete footing is modeled by elastic body, cast in place piles (reinforced concrete) by linear beam. The compressive strength of concrete was assumed to be 24 N/mm^2, Young's modulus 25 kN/mm^2, Poisons ratio 0.2, respectively. The height and natural period of first mode of each transmission tower are shown in Table 4.

Table 3. Specification of Pile Foundations of Transmission Tower

Items	Tower No.2	Tower No.3
Dimension of Footing	14.8m×14.8m	12.8m×12.8m
Thickness of Footing	2.0m	1.6m
Types of Piles	Cast in Place Pile (RC)	Cast in Place Pile (RC)
Number of Pile	8	12
Pile Diameter	1200 mm	1200 mm
Pile Bottom Depth	GL-12.50m	GL- 9.50m
Ground Surface Elevation	EL+249m	EL+254m
Vs30 value of surrounding ground	160m/s to 200m/s	250m/s to 350m/s

Table 4. Natural Period of Transmission Towers

Items	Tower No.2	Tower No.3
Height	74m	44m
Natural Period of the First Mode	0.59 sec	0.29 sec
Damping Ratio	0.02	0.02

Tower is simply modeled as single spring-mass system of which natural period is equivalent to the natural period of first mode of tower. The mass is specified from weight of tower itself excluding the weight of electric wires. The height of mass is simply assumed as one third of total height.

4.3 Finite Element Model of Soil Foundation System

Foundation and surrounding ground were modeled by three dimensional finite elements considering detailed shape of footing and piles. The FE model for tower no.3 is illustrated in Figure 8 as a typical example. Soil layer was assumed as horizontally layered deposit. The width and breadth of ground was determined as 90m, which was more than five times of the foundation width. The elevation of the bottom of model was unified to be EL+232.0m for both models. The side viscous boundary was defined at each side of the model to perform the same seismic behavior as free field at its edge. The bottom viscous boundary was defined as well through which outcrop input motion could be applied from the bottom.

In order to consider the volume of pile (Diameter of 1200mm) which was modeled by beam element, the cylindrical shape was precisely modeled in finite element mesh of ground. In this model, nodes at pile center were connected with nodes at outer surface of pile by rigid beam. The tower was modeled as single spring-mass model on the footing of foundation.

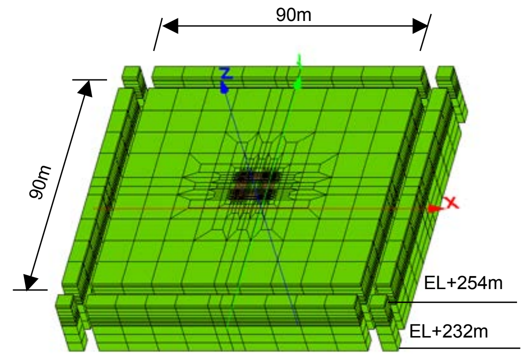

(a) Surrounding Ground and Foundation

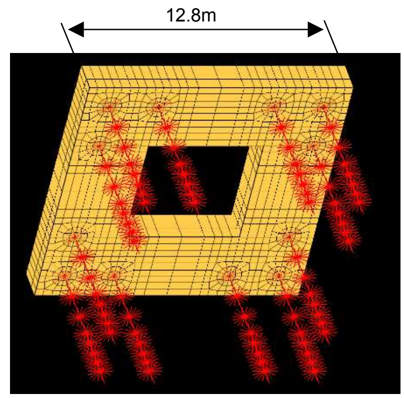

(b) Footing and Piles (Number of pile : 12)

Figure 8. Three Dimension Finite Element Model (Foundation of Tower No.3)

4.4 Reproduction of Ground Motion

The earthquake motion at the bottom of each model was reproduced using observed accelerations at the surface of recording station K-NET Kofu (YMN005, 2011/03/11-14:46, 38.103N, 142.860E, M9.0, NIED). Location of recording stations was about 7km north from the site. The outline of ground model used for reproduction calculation presented in Figure 9, recorded and reproduced peak ground accelerations in Table 5. The model from the surface to GL-20m was developed using borehole data at the recording station by NIED, and the model from GL-20m to the base of GL-37.7m by borehole data of deep subsoil structure investigation (Yamanashi Prefecture, 2005), which was located 800m south from recording station. Degradation of shear modulus and damping ratio with shear strain was specified based on a past study (Yamanashi Prefecture, 2005). The calculation was conducted using a one dimensional equivalent linear earthquake response analysis based on multiple reflection theory. The acceleration time histories were extracted at two points of A (Vs=210m/s) and B (Vs=420m/s) in Figure 9. The reproduced acceleration time histories at outcrop of Vs=420m/s are illustrated in Figure 10, response spectrum of horizontal accelerations in Figure 11. The peak base horizontal accelerations resulted in about 50 gal at the base of point B (Vs=420m/s), and about 70gal at the point A (Vs=210m/s).

Figure 12 illustrates time histories of accelerations at the layer of Vs=210m/s (Point A, GL-17m) and Vs=420m/s (Point B, GL-37.7m) between 130 seconds and 140seconds. It is seen that acceleration from Point A is more amplified and slightly delayed from acceleration from Point B.

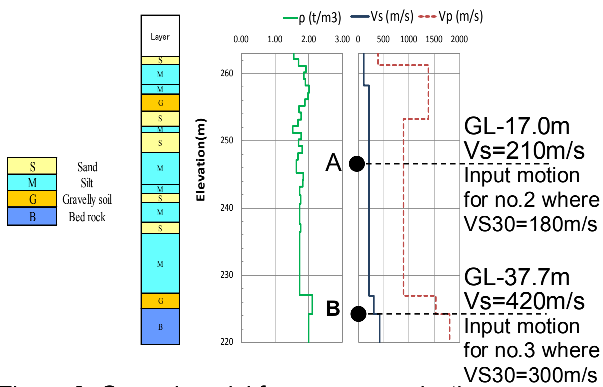

Figure 9. Ground model for wave reproduction

Table 5. Peak Ground Accelerations (Unit : gal)

Comp.	Recorded (Surface)	Reproduced (Vs=210m/s)	Reproduced (Vs=420m/s)
NS	64.1	60.3	45.2
EW	77.0	72.8	53.7
UD	29.9	31.1	25.4

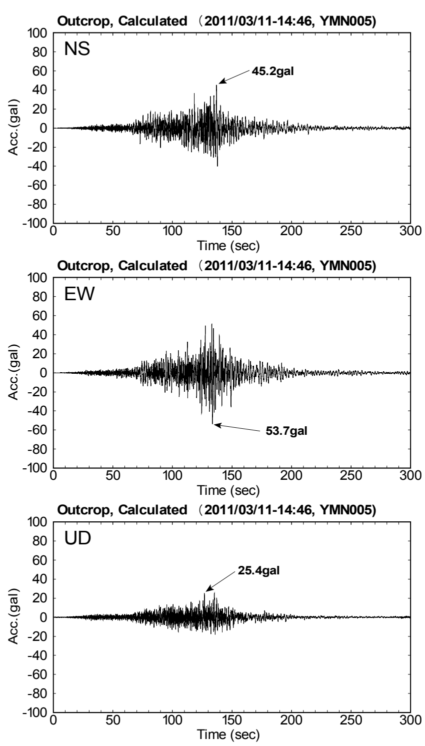

Figure 10. Time Histories of accelerations (Vs=420m/s)

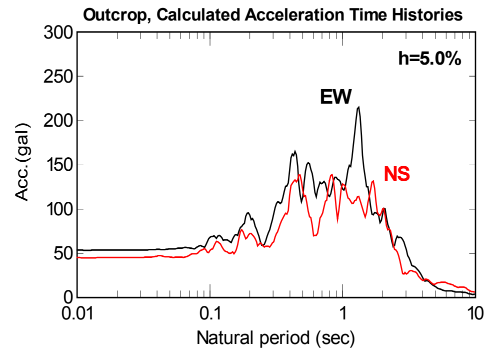

Figure 11. Acceleration Response Spectrum (Vs=420m/s)

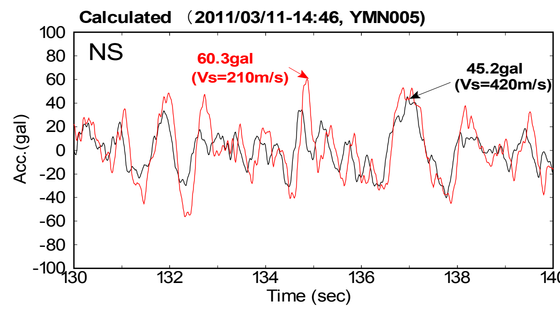

Figure 12. Time Histories of accelerations (2E, Vs=210m/s and Vs=420m/s)

4.5 Earthquake Response Analysis of Soil Foundation Coupled Model

Before the dynamic analysis, two stage of static analysis was conducted by gravity in order to simulate the initial stress of soil and initial section force in piles before the earthquake. First, gravity was applied to ground and foundation, and second, to the transmission tower. Horizontal displacement was constrained at side surface of ground model and both horizontal and horizontal displacement was fixed at the base through static analysis. With these initial conditions, an earthquake response analysis was conducted on the soil foundation coupled model. Three components of reproduced motion with duration time of 300 seconds were used simultaneously as the input motion. The analysis was conducted with undrained conditions (Iai, 1995) in order to simplify the analysis. The time integration was numerically done using the Wilson-θ method (θ=1.4) using a time step of 0.01 seconds. Reyleigh damping of α=0.0, β=0.001 was used to ensure stability of the numerical solution. The value of β for soil and foundation was determined considering initial natural period of first mode for ground model (no.2: 0.27s, no.3: 0.33s). It was assumed that initial damping ratio was 0.01. Reyleigh damping for tower of β_{stru}=0.004 for no.2, β_{stru}=0.002 for no.3 was used individually so that it became equivalent to damping of tower (h=0.02). Input motion from GL-17m (Vs=210) was applied to the model of tower no.2 in which shear wave velocity at the bottom of the model is specified as 210m/s. Input motion from GL-37m (Vs=420) was applied to the model of tower no.3.

4.6 Results of the Analysis

The effective stress dynamic analysis results in the maximum ratio of effective stress decrease ($1\text{-}\sigma_m'/\sigma_{m0}'$) and maximum shear strain γ_{oct}, through the whole duration time as illustrated in Figure 13 and Figure 14. It is observed that pore water pressure increased at subsoil around tower no.2 up to about ratio of 0.2. The maximum strain is observed to be the order of 10^{-3} in subsoil around tower no.2 foundation in which VS30 value is much lower.

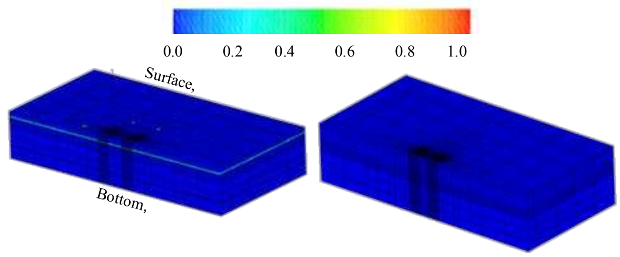

(a) Tower No.2 (b) Tower No.3

Figure 13. Maximum Ratio of effective stress decrease ($1\text{-}\sigma_m'/\sigma_{m0}'$, 0.0sec - 300.0 sec)

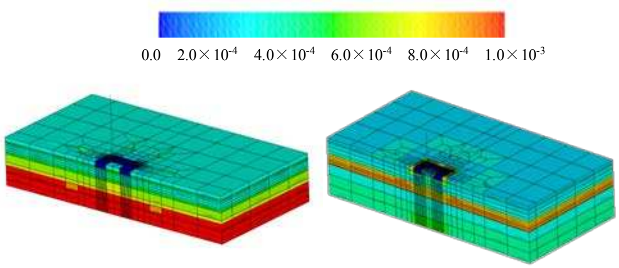

(a) Tower No.2 (b) Tower No.3

Figure 14. Maximum shear strain (γ_{oct}, 0.0sec - 300.0 sec)

Figure 15 illustrates the calculated horizontal acceleration time histories for whole duration at the top of foundation, Figure 16 for time period when amplitude of acceleration is significant. It is noted that the peak of acceleration time history of tower no.2 is slightly, about 0.2 seconds, delayed from the peak of no.3. This is because that initial shear stiffness of subsoil around foundation no.2 is smaller than that of no.3, also becomes soft during the earthquake due to build-up of excess pore water pressure and large shear strains.

Vertical displacement time histories at each foot of the same foundation are compared to examine the occurrence of rotation. Figure 17 illustrates tower no.2 and tower no.3, representing blue line as north foot, red line as south foot at the same foundation. It is observed in Figure 17 of tower no.2 that time histories are reversed each other, implying phase difference of about 180 occurs. This means the foundation no.2 dynamically rotates during earthquake. On the other hand in Figure 17 of tower no.3, significant difference of vertical displacement is not apparent, implying almost no rotation at foundation no.3. Figure 18 depicts time histories of rotation angle at each foundation.

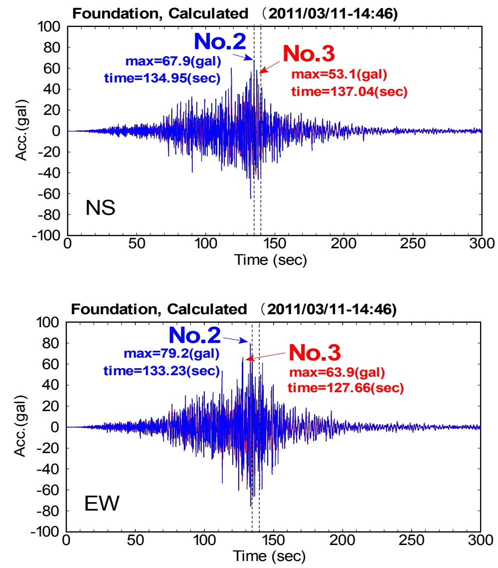

Figure 15. Calculated Time Histories (0.0sec - 300.0sec)

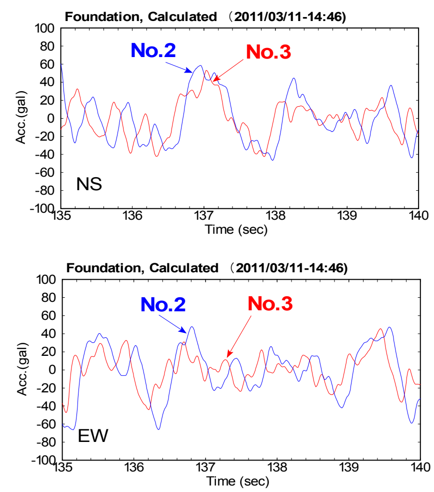

Figure 16. Calculated Time Histories (135.0sec–140.0sec)

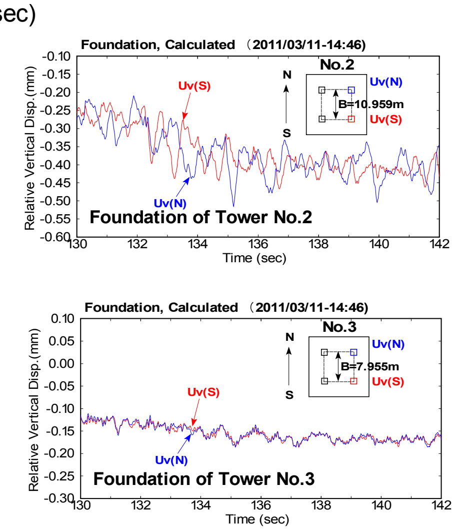

Figure 17. Vertical displacements (NS-comp.)

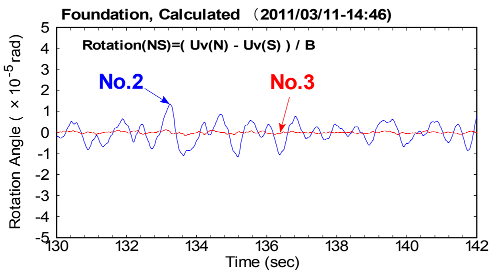

Figure 18. Rotation angle of foundations

It is apparently seen that foundation no.2 dynamically rotates more significantly than foundation no.3. This is due to difference of ground stiffness condition and number of pile between foundations (foundation no.2, VS30=180m/s, no. of pile=8, foundation no.3, VS30=300m/s, no. of pile=12).

5 CONCLUSIONS

The present study explained about ground conditions around the transmission towers and dynamic effective stress analysis of tower foundations to examine different earthquake response between foundations. The study leads to the following conclusions.

(1) Examining the ground conditions based on literature, it was cleared that subsoil condition at each tower foundation were obviously different regarding the average shear wave velocity of VS30 value and liquefaction potential.

(2) According to the case study by three dimensional dynamic effective stress analysis considering the Earthquake 3.11, phase difference of horizontal acceleration about 0.2 seconds were reproduced between foundations.

(3) Also it was found that more significant dynamic rotation was calculated in foundation no.2. We think occurrence of phase difference and relatively significant rotation at foundation no.2 are due to small initial ground stiffness, less number of piles, large mass and height of tower no.2.

(4) Different earthquake response between foundations in terms of horizontal motion and rotation are successfully reproduced considering ground condition and foundation at each tower.

For further study, followings may be important to clarify the difference of earthquake response between transmission towers;

- To consider local ups and downs of ground surface around foundations, especially due to existing river dikes and creeks around tower no.2.
- To take deeper part of ground properties, more than about GL-30m, into account. Basin terrain and deep subsoil structure as well.

ACKNOWLEDGEMENT: The authors express their gratitude to TEPCO Power Grid, Incorporated for providing authors such valuable data and information related to subsoil and foundations of transmission towers.

REFERENCES:

ADINA R&D,Inc. 2011: ADINA User Interface Command Reference Manual Volume 1: *ADINA Soils & Structures Model Definition.*

Disaster Management, Cabinet Office, Japan. 2001. *Report of Earthquake Damage Estimation due to the Tokai Earthquake, 10th conference, Nov.27th, 2001*, Handout 2-2: 11.

Iai, S., Matsunaga, Y., Kameoka, T. 1992. Strain Space Plasticity Model for Cyclic Mobility, *Soils and Foundations*, 32(2): 1–15.

Iai S. 1993. Three dimensional formulation and objectivity of a strain space multiple mechanism model for sand, *Soils and Foundations*, .33(1): 192-199.

Iai S. 1995. Response of a Dense Sand Deposit during 1993 Kushiro-oki Earthquake, *Soils and Foundations*, .35(1): 115-131.

Iai S., Tobita T., Ozutsumi O. and Ueda K. 2011. Dilatancy of granular materials in a strain space multiple mechanism model, *International Journal for Numerical and Analytical Methods in Geomechanics*, *Int. J. Numer. Anal. Meth. Geomech*. 35: 360-392.

Iwasaki, T., Tokida, K., Tatsuoka, F. 1981: Soil Liquefaction Potential Evaluation with use of the Simplified Procedure, *Proc. 1st Intl. Conf. of Recent Advances in Geotechnical Earthquake Engineering and Soil Dynamics, St. Louis, Missouri.*

Ministry of Land, Infrastructure, Transport and Tourism. 2016, Search Engine for National Land Geoinformation “Kunijiban”, http://www.kunijiban.pwri.go.jp/jp/index.html. (in Japanese)

Morita T., Iai S., Liu H., Ichii K., Sato Y., 1997. Simplified Method to Determine Parameter of FLIP, *Technical Note of the Port and Harbour Research Institute, Ministry of Transport, Japan*. (in Japanese)

National Research Institute for Earth Science and Disaster Prevention (NIED). “K-NET WWW service”, Japan (http://www.k-net.bosai.go.jp/).

National Research Institute for Earth Science and Disaster Prevention (NIED). “Japan Seismic Hazard Information Station (J-SHIS)”. 2016. (http://www.j-shis.bosai.go.jp/).

Ohta, H., Kawahara, A., Nakamura, H., Yamazaki, M., Hongo, E. 2014. Reproduction Analysis of Short-circuit between Transmission Lines during the 2011 Off the Pacific Coast of Tohoku Earthquake and a Consideration of the cause of the Event. *IEEJ Transactions on Power and Energy*, 134(8): 732-742. (in Japanese)

Yamanashi Prefecture, Japan. 2003: Survey of Deep Subsurface Structure Beneath Kofu basin. (in Japanese)

Yamanashi Prefecture, Japan. 2005: Report of Earthquake Damage Estimation due to the Tokai Earthquake in Yamanashi Prefecture. (in Japanese)

Yamanashi Prefecture, Japan. 2013: Report of Liquefaction Evaluation in Yamanashi Prefecture. (in Japanese)